AIAA 80-1369R

Numerical Solution of Three-Dimensional Unsteady Transonic Flow over Swept Wings

C. J. Borland,* D. P. Rizzetta,† and H. Yoshihara‡
Boeing Military Airplane Company, Seattle, Wash.

An algorithm for the calculation of unsteady transonic flow over three-dimensional swept wings undergoing general unsteady motion has been developed. The equation considered is the transonic small-disturbance potential equation with second-order terms to insure proper swept shock jump conditions. An alternating direction-implicit approximate factorization difference scheme is employed. A shearing transformation of the coordinates is applied in order to map a swept-tapered planform onto a rectangle in the computational domain. Use of a rotated type-dependent differencing scheme provides computational stability as well as proper shock capture. Computed results for an infinite-yawed wing are found to agree with two-dimensional solutions when simple sweep theory is applied for both the steady and unsteady cases. Steady three-dimensional results compare favorably with existing steady methods. Unsteady results are presented for a swept wing undergoing sinusoidal pitching motion at $M=0.9$. It is found that the shock position oscillates over about 16% of chord at the wing tip.

Nomenclature

a	$=(1/c)(E+2G_s c\xi_y\phi_\eta)$
b	$=(1/c)(F+G_s c^2\xi_y^2)$
B	$=2M^2k$
c	= local section chord nondimensionalized by c_r
c_r	= reference chord
C_l	= wing lift coefficient ($2\times$lift$/\rho U^2$)
C_m	= wing moment coefficient ($2\times$moment$/\rho U^2$)
C_p	= local section pressure coefficient
D	= type-dependent difference operator
E	$=1-M^2$
f	= local instantaneous section definition, i.e., $z=f(x,t)$
f_0	$=-B\phi_x$
f_1	$=E\phi_x+F\phi_x^2+G\phi_y^2$
f_2	$=\phi_y+H\phi_x\phi_y$
f_3	$=\phi_z$
F	= see Eqs. (4a) and (5a)
g	= initial ϕ distribution
G	= see Eqs. (4b) and (5b)
H	= see Eqs. (4c) and (5c)
k	= reduced frequency $\omega c_r/U$
M	= freestream Mach number
t	= time nondimensionalized by $1/\omega$
U	= freestream velocity
x	= physical streamwise coordinate nondimensionalized by c_r
X	= see Eq. (14c)
y	= physical spanwise coordinate nondimensionalized by c_r
Y	= see Eq. (14d)
z	= physical normal coordinate nondimensionalized by c_r
α	= instantaneous angle of attack
γ	= specific heat ratio
Δt	= time step size
δ	= difference operator
ζ	= nondimensional transformed normal coordinate
η	= nondimensional transformed spanwise coordinate
Λ	= wing sweep angle
ξ	= nondimensional transformed streamwise oordinate
ρ	= freestream density
τ	= airfoil section thickness
ϕ	= perturbation velocity potential function nondimensionalized by c_rU
Φ	= physical velocity potential function, i.e., $c_rU(x+\phi)$
ω	= oscillation frequency

Superscripts

$(\ )^+$	= upper surface
$(\ )^-$	= lower surface
$(\overleftarrow{\ })$	= backward difference
$(\tilde{\ })$	= first intermediate solution (prediction)
$(\tilde{\tilde{\ }})$	= second intermediate solution (first correction)
n	= previous time level
$n+1$	= final solution at new time level (second correction)

Subscripts

2D	= two-dimensional
3D	= three-dimensional
le	= leading edge
min	= minimum
N	= normal direction
S	= streamwise direction
t	= time derivative
te	= trailing edge
tip	= wing tip
x,y,z,ξ,η,ζ	= spatial derivative

Presented as Paper 80-1369 at the AIAA 13th Fluid and Plasma Dynamics Conference, Snowmass, Colo., July 14-16, 1980; submitted Aug. 12, 1980; revision received Aug. 20, 1981. Copyright © American Institute of Aeronautics and Astronautics, Inc., 1980. All rights reserved.

*Principal Engineer. Associate Fellow AIAA.
†Senior Specialist Engineer. Member AIAA.
‡Engineering Manager. Fellow AIAA.

Introduction

THE most difficult and most dangerous problems in aircraft aeroelasticity arise in the transonic flight regime. Some aircraft, during their development phase, have experienced aeroelastic difficulties in transonic flight which have not been adequately predicted by traditional aeroelastic analysis. This situation has arisen because of two factors: 1) the nonlinearity of the unsteady transonic flow equations; and 2) the appearance of unsteady shock waves on the wing and their interaction with the boundary layer, causing large

changes in the unsteady aerodynamic forces. During the last decade there has been considerable progress in formulating numerical methods for the solution of steady and unsteady transonic flow problems. Magnus and Yoshihara[1] demonstrated the feasibility of numerical solution of the Euler equations for inviscid steady flow over a two-dimensional airfoil at transonic speed. Their work was later extended[2] to unsteady flow, but computation times were considered prohibitive for practical calculations. Murman and Cole[3] solved the two-dimensional, steady, small-disturbance potential equation for transonic flow, showing that the essential features of the problem, i.e., mixed subsonic-supersonic flow regions and the presence of shock waves, could be simulated by a simple mathematical model. References 4-8 have extended this work to full three-dimensional, steady, small-disturbance solutions for aircraft configurations including bodies, nacelles, and winglets. Solutions of the more complete full-potential equation have been described in several papers.[9,10] These have generally proven more difficult to obtain because of the additional complexity of satisfying the surface boundary conditions exactly. In the small-disturbance methods, a linearized boundary condition is usually satisfied on a mean chord plane. Because of this simplicity, and the desire to develop a practical aeroelastic computation tool at reasonable computer costs, these methods have been chosen for the work described herein.

Two basic approaches to the unsteady transonic flow problem presently exist. These are classified as "frequency-expansion" or "time-linearized" methods[11-14] and nonlinear "time-integration" methods.[15] The frequency expansion method assumes that the unsteady flowfield may be considered as a linear perturbation about a mean steady state. Resulting shock waves are thereby constrained to remain fixed at their steady-state location. In addition, time variation of the linear perturbation is commonly assumed to be harmonic. Experimental evidence[16] has shown several classes of unsteady transonic flow which do not exhibit this simple behavior. Also, until recently[17] these methods have been limited by numerical difficulties to very low frequency motions.

The alternate approach of time integration removes many of the limitations of the frequency expansion method. Most importantly, the motion of shock waves can be accurately predicted. Reference 15 demonstrated the ability of the method to reproduce the various types of irregular shock motion that have been observed experimentally. From an aeroelastic viewpoint, there has been considerable discussion[18] about the importance of shock motion in transonic aeroelastic stability, thus evidencing an urgent need for a method which accounts for these effects. Additional attractive features of the method are the ability to handle general unsteady (rather than sinusoidal) motion, the incorporation of nonlinear effects of finite motion amplitude, and the removal of frequency limitations, provided the proper time-dependent terms are included in the formulation.[19] In aeroelastic calculations it will be possible to couple the aerodynamic and structural solutions directly, rather than the indirect and expensive approach of calculating aerodynamics for each structural mode shape and frequency independently.

To date, no practical extension of the time integration method to three-dimensional unsteady flow about wings has been made. Some work concerning helicopter blade aerodynamics has been reported.[20,21] Extensions of more complex representations, such as full-potential solutions, to unsteady flows are now becoming available for the two-dimensional case,[22,23] but are still in an early state of development. Thus the most practical method for performing three-dimensional unsteady transonic aeroelastic analysis of wings appears to be the method of time integration of the small-disturbance equations. This approach can incorporate much of the complexity of the three-dimensional steady methods[5] necessary to obtain accurate solutions of thin clean wings. In addition, this technique can be extended to more complex configurations by the method of Ref. 8.

Governing Equation

The governing equation to be considered is the low-frequency approximation to the modified three-dimensional unsteady transonic small-disturbance equation given in conservative form as:

$$\frac{\partial f_0}{\partial t}+\frac{\partial f_1}{\partial x}+\frac{\partial f_2}{\partial y}+\frac{\partial f_3}{\partial z}=0 \tag{1}$$

where

$$f_0=-B\phi_x \tag{2a}$$

$$f_1=E\phi_x+F\phi_x^2+G\phi_y^2 \tag{2b}$$

$$f_2=\phi_y+H\phi_x\phi_y \tag{2c}$$

$$f_3=\phi_z \tag{2d}$$

Here ϕ is the small-disturbance potential defined by $\Phi=c_r U(x+\phi)$ with

$$B=2M^2k \tag{3a}$$

$$E=1-M^2 \tag{3b}$$

Three separate forms for the remaining constants F, G, and H may be considered. A steady, three-dimensional equation analogous to Eq. (1) was proposed by Lomax et al.[5] with the coefficients defined as:

$$F=-\tfrac{1}{2}(\gamma+1)M^2 \tag{4a}$$

$$G=\tfrac{1}{2}(\gamma-3)M^2 \tag{4b}$$

$$H=-(\gamma-1)M^2 \tag{4c}$$

These will be referred to as the NASA/AMES coefficients. An alternative version was suggested by Van der Vooren et al.[24]:

$$F=-\tfrac{1}{2}[3-(2-\gamma)M^2]M^2 \tag{5a}$$

$$G=-\tfrac{1}{2}M^2 \tag{5b}$$

$$H=-M^2 \tag{5c}$$

These will be referred to as the NLR coefficients. If, on the other hand, F is considered given by Eq. (4a) and $G=H=0$ the classical form of the equation is recovered. In Ref. 5 it was pointed out that the additional "cross terms" proportional to G and H were necessary to correctly capture swept shocks for wings with sweep angle greater than approximately 15 deg. The NLR coefficients were shown to have improved properties for the capture of the highly swept forward shock.

Boundary Conditions

A formal definition of the problem is completed by the boundary conditions:

Far upstream:

$$\phi=0 \tag{6a}$$

Far downstream:

$$\phi_x=0 \tag{6b}$$

Wing root:

$$\phi_y = 0 \tag{6c}$$

Far spanwise:

$$\phi_y = 0 \tag{6d}$$

Far above and below:

$$\phi_z = 0 \tag{6e}$$

On the wing surface the following linearized unsteady boundary condition has been applied:

$$\phi_z^{\pm} = f_x^{\pm} + k f_t^{\pm} \tag{6f}$$

on

$$z = 0^{\pm} \quad \text{for } x_{le} \le x \le x_{te} \tag{6g}$$

Across the trailing vortex sheet in the wake defined by $z=0$ for $x > x_{te}$ the contact conditions

$$[\phi_z] = 0 \quad \text{(continuity of slope)} \tag{7a}$$

$$[\phi_x] = 0 \quad \text{(continuity of pressure)} \tag{7b}$$

are applied where the brackets denote the jump in the enclosed quantity from above to below the vortex sheet. Finally, the problem is fully defined by specification of the initial condition

$$\phi(x,y,z,0) = g(x,y,z) \tag{8}$$

Transformation of Coordinates

The following shearing transformation is applied in order to map a swept-tapered wing planform in the physical domain into a rectangular wing in the Cartesian computational domain:

$$\xi = \frac{x - x_{le}(y)}{c(y)} \qquad \eta = y \qquad \zeta = z \tag{9}$$

Outboard of the wing tip, the mapping applies a smooth transition to a constant chord section swept at the average of the leading and trailing edge sweep angles in the manner of Ref. 7. This results in the following conservation form of the governing equation:

$$-\frac{\partial}{\partial t}(B\phi_\xi) + \frac{\partial}{\partial \xi}\left[\left(\frac{E}{c}\right)\phi_\xi + \left(\frac{F}{c^2}\right)\phi_\xi^2 + G(\xi_y\phi_\xi + \phi_\eta)^2 + c\xi_y(\xi_y\phi_\xi + \phi_\eta) + H\xi_y\phi_\xi(\xi_y\phi_\xi + \phi_\eta)\right] + \frac{\partial}{\partial \eta}[c(\xi_y\phi_\xi + \phi_\eta) + H\phi_\xi(\xi_y\phi_\xi + \phi_\eta)] + \frac{\partial}{\partial \zeta}[c\phi_\zeta] = 0 \tag{10}$$

The coefficient G is now split into two components

$$G = G_s + G_N \tag{11}$$

such that Eq. (10) may be decomposed into streamwise and normal contributions to the spatial differencing. Thus,

$$\frac{\partial}{\partial_\xi}\left[\left(\frac{E}{c}\right)\phi_\xi + \left(\frac{F}{c^2}\right)\phi_\xi^2 + G_s(\xi_y\phi_\xi + \phi_\eta)^2\right] \tag{12}$$

represents the streamwise portion of Eq. (10), and the remaining terms comprise the normal contribution where

$$G_s = 1 - M^2$$

This decomposition will allow all streamwise spatial differences to be treated implicitly and thereby enhance stability.

At this point it is convenient to recast the governing equation in a form that is more practical for numerical solution. For this purpose, it is necessary to treat some of the terms nonconservatively. The reasons for this will subsequently become apparent. Equation (10) is now written as:

$$B\phi_{\xi t} = \frac{\partial}{\partial \xi}\left[\left(\frac{E}{c}\right)\phi_\xi + \left(\frac{F}{c^2}\right)\phi_\xi^2\right] + \frac{\partial}{\partial \xi}[G_s(\xi_y\phi_\xi + \phi_\eta)^2] + \frac{\partial}{\partial \xi}[G_N(\xi_y\phi_\xi + \phi_\eta)^2 + c\xi_y(\xi_y\phi_\xi + \phi_\eta) + H\xi_y\phi_\xi(\xi_y\phi_\xi + \phi_\eta)] + \frac{\partial}{\partial \eta}[c(\xi_y\phi_\xi + \phi_\eta) + H\phi_\xi(\xi_y\phi_\xi + \phi_\eta)] + \frac{\partial}{\partial \zeta}[c\phi_\zeta] \tag{13}$$

Upon defining

$$a = \left(\frac{1}{c}\right)(E + 2G_s c\xi_y\phi_\eta) \tag{14a}$$

$$b = \left(\frac{1}{c^2}\right)(F + G_s c^2 \xi_y^2) \tag{14b}$$

$$X = G_N(\xi_y\phi_\xi + \phi_\eta)^2 + H\xi_y^2\phi_\xi^2 + H\xi_y\phi_\xi\phi_\eta + c\xi_y\phi_\eta + c\xi_y^2\phi_\xi \tag{14c}$$

$$Y = H\xi_y\phi_\xi^2 + H\phi_\xi\phi_\eta + c\xi_y\phi_\xi \tag{14d}$$

Eq. (13) becomes

$$B\phi_{\xi t} = \frac{\partial}{\partial \xi}(a\phi_\xi + b\phi_\xi^2) + 2G_s\phi_\eta\phi_{\xi\eta} + \frac{\partial}{\partial \eta}(c\phi_\eta) + c\frac{\partial^2\phi}{\partial \zeta^2} + \frac{\partial X}{\partial \xi} + \frac{\partial Y}{\partial \eta} \tag{15}$$

The shearing transformation effects the boundary conditions as follows:

Far upstream:

$$\phi = 0 \tag{16a}$$

Far downstream:

$$\frac{1}{c}\phi_\xi = 0 \tag{16b}$$

Wing root:

$$\xi_y\phi_\xi + \phi_\eta = 0 \tag{16c}$$

Far spanwise:

$$\phi_\eta = 0 \tag{16d}$$

Far above and below:

$$\phi_\zeta = 0 \tag{16e}$$

Wing surface:

$$\phi_\zeta^{\pm} = \frac{1}{c}f_\xi^{\pm} + k f_t^{\pm} \quad \text{on } \zeta = 0^{\pm} \text{ for } 0 \le \xi \le 1 \tag{16f}$$

Vortex sheet:

$$[\phi] = 0 \tag{16g}$$

and

$$\left[\frac{1}{c}\phi_\xi\right]=0 \qquad \text{on } \zeta=0 \text{ for } \xi>1 \tag{16h}$$

The initial condition becomes

$$\phi(\xi,\eta,\zeta,0)=g(\xi,\eta,\zeta) \tag{16i}$$

The wing root boundary condition applied in the transformed plane requires some special treatment due to the appearance of both streamwise and spanwise derivatives. Equation (16c) may be satisfied by assuming a row of "dummy points" inboard of the wall and writing a finite-difference expression for the dummy point potential which satisfies the boundary condition at the wall mesh point. A similar approach was described in Ref. 6, except that there the boundary condition was satisfied at the dummy point instead of at the wall mesh point. Note that the far spanwise condition has been simplified for convenience.

Numerical Algorithm

The time-accurate solution to Eq. (15) may be obtained by the following first-order accurate (Δt) alternating direction-implicit algorithm:

1) ξ sweep

$$B\overleftarrow{\delta}_\xi\left(\frac{\tilde{\phi}-\phi^n}{\Delta t}\right)=D_\xi\left[a^n\left(\frac{\tilde{\phi}_\xi+\phi^n_\xi}{2}\right)+b\phi^n_\xi\tilde{\phi}_\xi\right]$$
$$+2G_s(\delta_\eta\phi^n)D_\eta(\overleftarrow{\delta}_\xi\phi^n)+\delta_\eta(c\delta_\eta\phi^n)$$
$$+c\delta_{\zeta\zeta}\phi^n+\delta_\xi X^n+\delta_\eta Y^n \tag{17a}$$

2) η sweep

$$B\overleftarrow{\delta}_\xi\left(\frac{\tilde{\tilde{\phi}}-\tilde{\phi}}{\Delta t}\right)=\tfrac{1}{2}\delta_\eta(c\delta_\eta\tilde{\tilde{\phi}}-c\delta_\eta\phi^n)$$
$$+G_s(\delta_\eta\phi^n)D_\eta(\overleftarrow{\delta}_\xi\tilde{\tilde{\phi}}-\overleftarrow{\delta}_\xi\phi^n) \tag{17b}$$

3) ζ sweep

$$B\overleftarrow{\delta}_\xi\left(\frac{\phi^{n+1}-\tilde{\tilde{\phi}}}{\Delta t}\right)=\frac{c}{2}\delta_{\zeta\zeta}(\phi^{n+1}-\phi^n) \tag{17c}$$

where δ_ξ, δ_η, and $\delta_{\zeta\zeta}$ are second-order central-difference operators, $\overleftarrow{\delta}_\xi$ is a first-order backward-difference operator, D_ξ is a mixed-difference operator based on the sign of $(a^n+2b\phi^n_\xi)$, and D_η is a mixed-difference operator based on the sign of $2G_s(\delta_\eta\phi^n)$. The form of the operator D_ξ is identical to the conservative mixed-difference operator D_x of Ref. 15, except that the streamwise portion of the cross term $[G\phi_y^2]_x$ appears in the mixed differencing. The spanwise mixed-difference operator D_η is treated as a forward difference for outward flow and a backward difference for inward flow. This maintains the diagonal dominance of the matrix solution and enhances stability, although the differencing is only first-order accurate. It should be noted that the streamwise terms proportional to G_s must be differenced nonconservatively if they are to be treated implicitly. Conservative differencing would require implicit treatment of ϕ_η on the ξ sweep which cannot be formulated in terms of simple matrix equations.

The three sweeps are solved for the intermediate values $\tilde{\phi}$ and $\tilde{\tilde{\phi}}$, and the final value ϕ^{n+1} of the updated velocity potential at time $t^{n+1}=t^n+\Delta t$. This entails a quadradiagonal matrix solution for the ξ sweep and tridiagonal solutions for the η and ζ sweeps. Since the ξ and η sweeps can be done sequentially in ξ-η planes for the entire computational domain before the ζ sweeps are performed, the first intermediate solution $\tilde{\phi}$ need not be stored for the complete three-dimensional mesh. Thus two "levels" of storage of ϕ^n and $\tilde{\tilde{\phi}}$ are required for the ζ sweep. Due to the backward operator $\overleftarrow{\delta}_\xi$, solutions in the η and ζ sweeps may proceed in the positive ξ direction. Thus the updated value ϕ^{n+1} can be overstored into the previous solution ϕ^n.

This algorithm is used to advance the solution for ϕ from time t (i.e., ϕ^n) to time $t+\Delta t$ (i.e., ϕ^{n+1}) at each interior point in the computational domain. All of the terms contributing to the streamwise portion of the equation are treated implicitly, as well as the second differences $\delta_\eta(c\delta_\eta\phi)$ and $c\delta_{\zeta\zeta}\phi$. The remaining cross terms contained in the expressions for X and Y are handled in an explicit manner. Because of this, there is an inherent time step limitation for stability of the three-dimensional code that is not present for fully implicit methods such as that of Ref. 15. For three-dimensional cases in which the magnitudes of cross terms are small, such as rectangular wing planforms, stability of the algorithm is comparable to that of Ref. 15. For cases with significant spanwise variation, such as swept-tapered wings, a much smaller time step (by a factor of three or four) must be used to maintain stability.

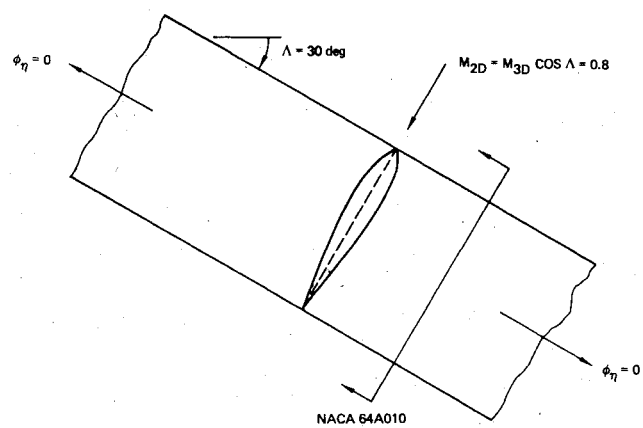

Fig. 1 Schematic of flow over an infinite yawed wing.

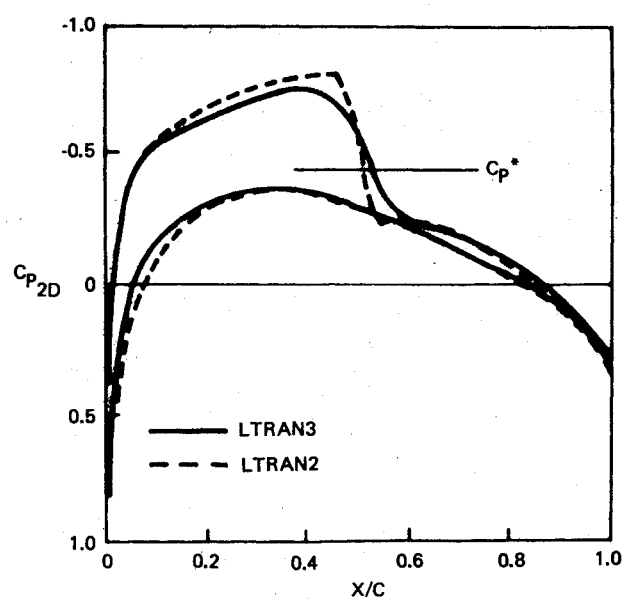

Fig. 2 Steady pressures for an infinite yawed wing and equivalent 2-D airfoil for $\alpha_{2D}=1$ deg, $M_{2D}=0.8$.

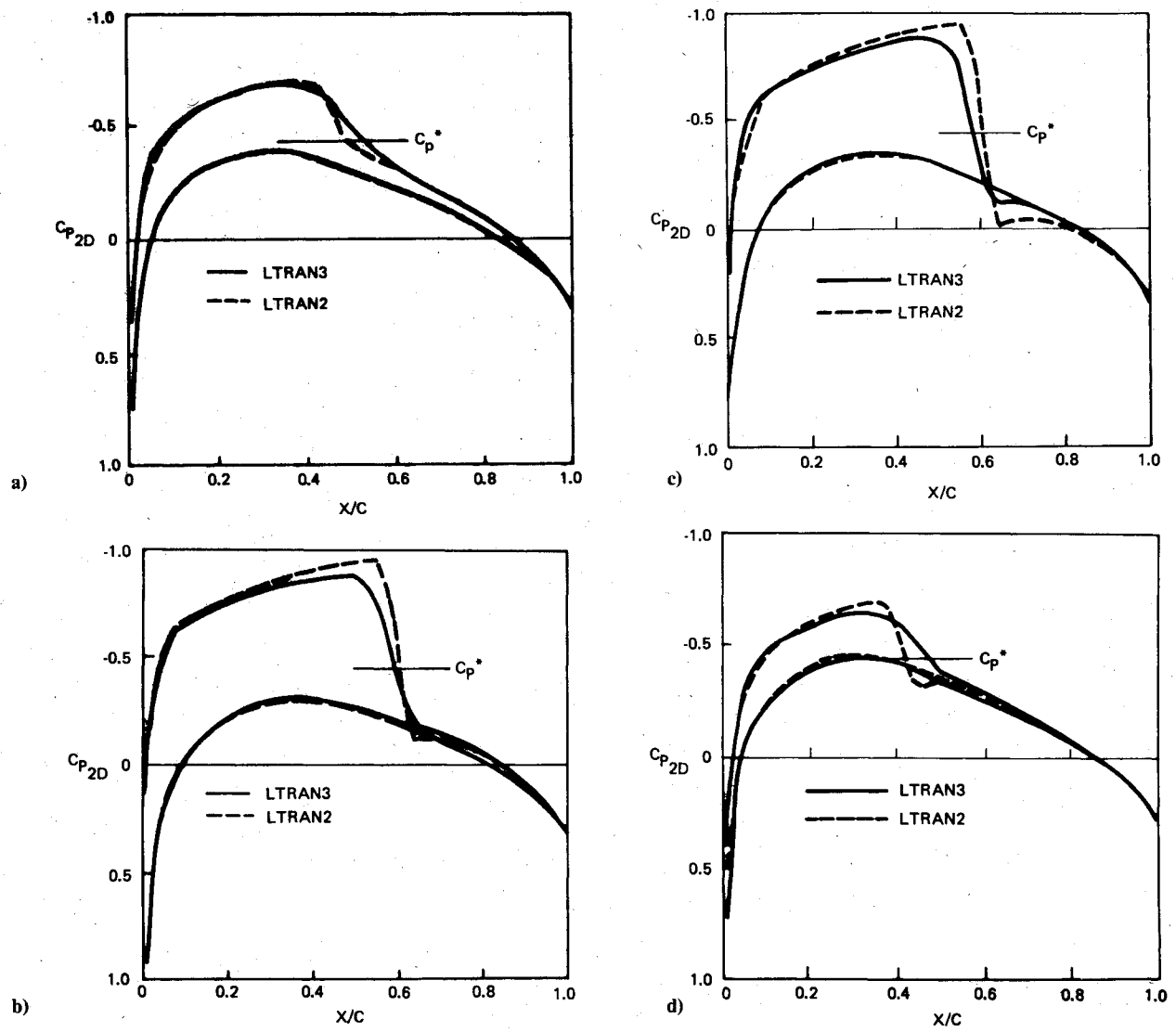

Fig. 3 Unsteady pressures for an infinite yawed wing and equivalent 2-D airfoil in sinusoidal pitching oscillation for $\alpha_{2D} = 1$ deg + 1 deg sin (t), $M_{2D} = 0.8$. a) $t = 0$, $\alpha_{2D} = 1$ deg; b) $t = \pi/2$, $\alpha_{2D} = 2$ deg; c) $t = \pi$, $\alpha_{2D} = 1$ deg; d) $t = 3\pi/2$, $\alpha_{2D} = 0$ deg.

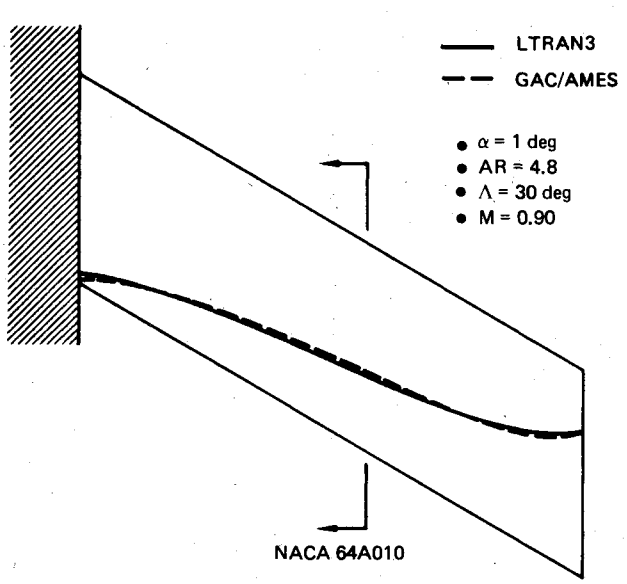

Fig. 4 Predicted shock location for steady flow about a swept wing.

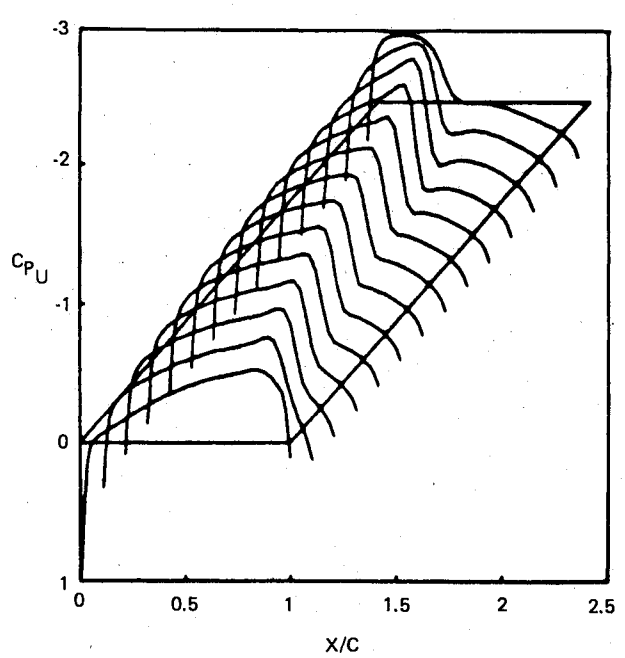

Fig. 5 Steady pressure distribution on the upper surface of a swept wing for $\alpha = 1$ deg.

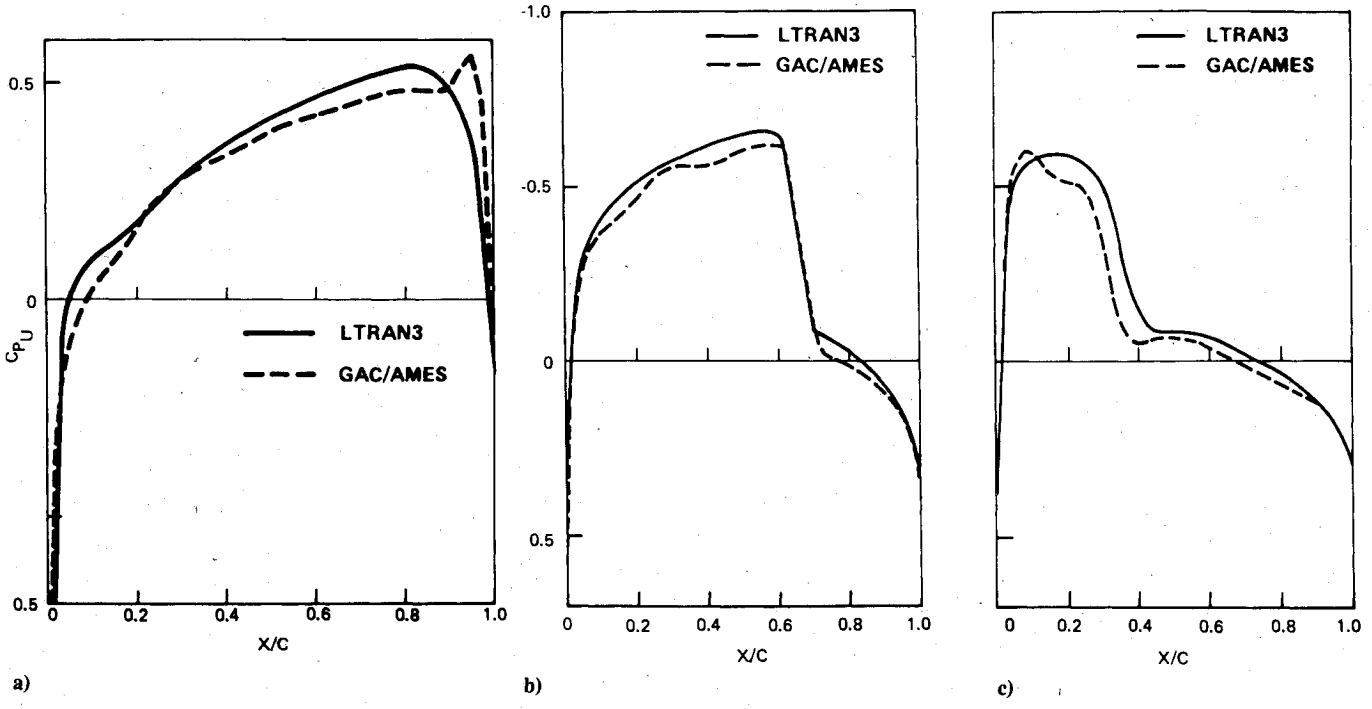

Fig. 6 Comparison of LTRAN3 and GAC/AMES code-calculated upper surface pressures. a) $\eta = 0.0$; b) $\eta = 1.07$, $\eta/\eta_{tip} = 0.44$; c) $\eta = 2.40$, $\eta/\eta_{tip} = 0.98$.

Computed Results

The numerical algorithm described above has been incorporated in the computer code LTRAN3 written for the CDC 7600 computer. All of the three-dimensional results presented here were computed on a coarse nonuniform $60 \times 20 \times 40$ (ξ, η, ζ) computational mesh with the wing surface defined by 39×12 of these points in the ξ-η plane. The minimum grid spacings and computational boundaries are given as:

$$\Delta\xi_{min} = 0.01, \qquad \Delta\eta_{min} = 0.25, \qquad \Delta\zeta_{min} = 0.025$$

$$-12.775 \leq \xi \leq 26.575$$

$$0 \leq \eta \leq 5.0 \text{(wing tip at } \eta = 2.45)$$

$$-13.0375 \leq \zeta \leq 13.0375$$

With this mesh 3 s of CPU time (CDC 7600) were required for each time step (3 sweeps).

In order to assess the accuracy of the capture of swept shocks, LTRAN3 has been used to calculate the flow about an infinite aspect ratio yawed wing, illustrated schematically in Fig. 1. The wing has an NACA 64A010 airfoil section in the plane normal to the swept leading edge. The steady flow at a constant mean angle of attack and the unsteady flow for an oscillatory angle of attack about the mean position have been calculated. For comparison purposes, the flow about the equivalent two-dimensional airfoil has been calculated using the LTRAN2[15] code. The following set of sweep theory relationships gives the flow parameters and the equivalence between the two- and three-dimensional calculations.

$$\text{For } \Lambda = 30 \text{ deg}, \; M_{2D} = 0.8, \; \alpha_{2D} = 1 \text{ deg} + 1 \text{ deg} \sin t$$

$$M_{3D} = M_{2D}/\cos\Lambda = 0.9237$$

$$\tau_{3D} = \tau_{2D}\cos\Lambda = 0.0866$$

$$\alpha_{3D} = \alpha_{2D}\cos\Lambda = 0.866 + 0.866 \sin t$$

$$C_{p_{3D}} = C_{p_{2D}}\cos^2\Lambda$$

Figure 2 gives the steady upper and lower surface pressures as calculated by the two programs and scaled to give equivalence by the relationships above. It may be seen that the shock strength (total pressure jump) and location are correctly predicted by the three-dimensional calculation, but some additional smearing of the captured oblique shock occurs. A relatively coarse grid has been used for both calculations. All spanwise effects on the swept wing have been suppressed by forcing $\phi_\eta = 0$ at both side boundaries of the computational mesh. The same comparison is made in Figs. 3a-d and for a pitching oscillation at a reduced frequency of 0.2 based on chord. This is a relatively severe case and involves rapid motion of the shock over about 20% of the chord. Pressures are shown every 90 deg of phase of the unsteady oscillation starting from a previously established periodic flow. Except for the shock smearing noted above, the comparison of three-dimensional calculations is good. At the maximum strength and maximum rearward excursion of the shock (Fig. 3c), it may be noted that the three-dimensional calculation predicts a slightly weaker shock located about 3% forward. This may be due to nonconservative treatment of part of the cross term as described above.

The second case examined herein demonstrates the calculation of the transonic flow about a swept wing undergoing pitching oscillations. The planform of the wing and flow parameters are shown in Fig. 4, together with the steady state shock locations predicted by LTRAN3 and by a version of the Bailey-Ballhaus code,[7] hereafter referred to as GAC/AMES. This code has been shown to compare well with full-potential solutions and with experiment for wings of moderate thickness. The steady pressure distribution on the wing upper surface is shown in Fig. 5. Comparison of LTRAN3 results with those of the GAC/AMES code are

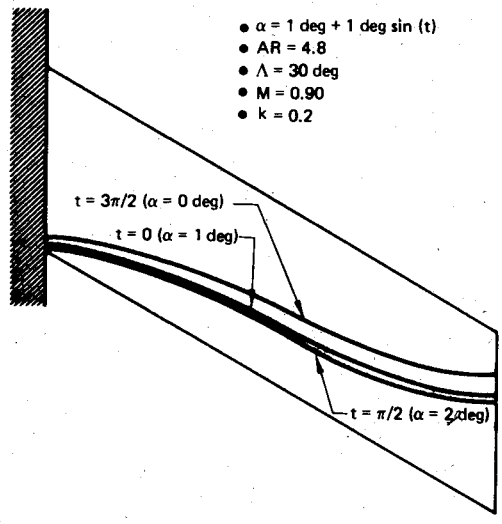

Fig. 7 Predicted shock location for unsteady flow about a swept wing oscillating in pitch.

shown for three spanwise stations in Figs. 6a-c. The two solutions predict essentially the same pressure distribution and shock location, although slight differences are attributed to details of the mesh spacing. The GAC/AMES result shown is for the embedded "fine grid"[6] which has approximately twice as many mesh points as LTRAN3.

Figure 7 shows the unsteady shock position calculated for a 1-deg pitching oscillation of the swept wing about the midpoint of the root chord. It may be seen that for this case, the steady-state characteristics of the shock are maintained, i.e., unsweeping near the root and tip and nearly two-dimensional flow in the center portion of the wing. The excursion of the oscillating shock is about 7% of chord near the root but nearly 16% of chord near the tip. Except for the last outboard station, the shock is present during the entire cycle of oscillation. This is the shock motion defined as type "A" by Tijdeman.[16] The three-dimensional, upper surface pressure distributions corresponding to these shock locations are shown in Figs. 8a-d.

Conclusions and Discussions

A method has been described for computing the unsteady transonic flow about thin wings of general planform. A more

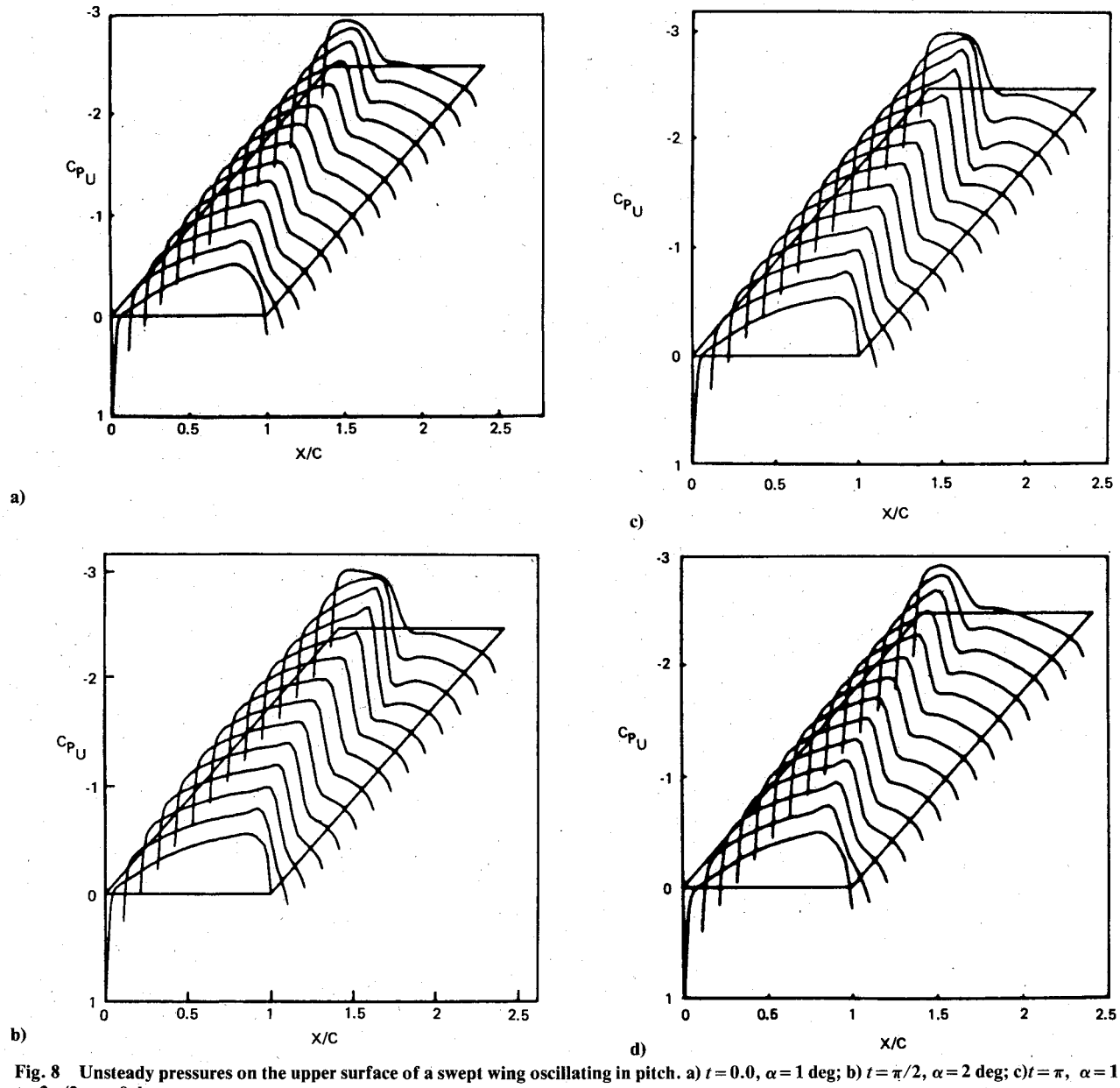

Fig. 8 Unsteady pressures on the upper surface of a swept wing oscillating in pitch. a) $t = 0.0$, $\alpha = 1$ deg; b) $t = \pi/2$, $\alpha = 2$ deg; c) $t = \pi$, $\alpha = 1$ deg; d) $t = 3\pi/2$, $\alpha = 0$ deg.

complete description of the details of this method may be found in Ref. 25. The governing equation was assumed to be that of "second-order," small-disturbance theory which retains the essential nonlinear nature of the transonic regime. Comparisons with two-dimensional steady and unsteady results using simple sweep theory and with steady calculations by an existing method indicate the validity of the solutions. Calculation of the unsteady flow over a swept wing has demonstrated the ability of the method to predict unsteady shock motions.

While the results presented herein are of a preliminary nature, LTRAN3 is capable of treating much more complex wing motions including movable control surfaces, general unsteady rigid body motions, and elastic deformations. This code may now be coupled with structural equations of motion for the prediction of aircraft flutter, gust loads, dynamic response, and other aeroelastic calculations. In addition, because of the efficient ADI algorithm, the method is readily adaptable to vector processing machines.

Acknowledgments

The authors are grateful to Dr. James J. Olsen, AFWAL/FDL and Dr. William F. Ballhaus, NASA/ARC for their useful suggestions. They also wish to thank Dr. Chen C. Sun of the Boeing Company for his help in comparisons with the GAC/AMES code. The work reported here was supported by the United States Air Force under Contract F33615-78-C-3201.

References

[1] Magnus, R. J. and Yoshihara, H., "Inviscid Transonic Flow Over Airfoils," AIAA Paper 70-47, Jan. 1970.

[2] Magnus, R. J. and Yoshihara, H., "Unsteady Transonic Flows Over an Airfoil," *AIAA Journal,* Vol. 13, Dec. 1975, pp. 1622-1628.

[3] Murman, E. M. and Cole, J. D., "Calculation of Plane Steady Transonic Flows," *AIAA Journal,* Vol. 9, Jan. 1971, pp. 114-121.

[4] Ballhaus, W. F. and Bailey, F. R., "Numerical Calculation of Transonic Flow About Swept Wing," AIAA Paper 72-677, June 1972.

[5] Lomax, H., Bailey, F. R., and Ballhaus, W. F., "On the Numerical Simulation of Three-Dimensional Transonic Flow with Application to the C-141 Wing," NASA TN D-6933, Aug. 1973.

[6] Boppe, C. W., "Calculation of Transonic Wing Flows by Grid Embedding," AIAA Paper 77-207, Jan. 1977.

[7] Mason, W., Mackenzie, D. A., Stern, M. A., and Johnson, J. D., "A Numerical Three-Dimensional Viscous Transonic Wing-Body Analysis and Design Tool," AIAA Paper 78-10, Jan. 1978.

[8] Boppe, C. W. and Stern, M. A., "Simulated Transonic Flows for Aircraft with Nacelles, Pylons, and Winglets," AIAA Paper 80-104, Jan. 1980.

[9] Jameson, A. and Caughey, D. A., "A Finite Volume Method for Transonic Potential Flow Calculations," AIAA Paper 77-635, June 1977.

[10] Holst, T. L., "A Fast Conservative Algorithm for Solving the Transonic Full-Potential Equation," AIAA Paper 79-1456, July 1979.

[11] Traci, R. M., Albano, E. D., and Farr, J. L., "Small Disturbance Transonic Flows About Oscillating Airfoils," AFFDL-TR-74-37, June 1974.

[12] Ehlers, F. E., "A Finite Difference Method for the Solution of the Transonic Flow Around Harmonically Oscillating Wings," AIAA Paper 74-543, June 1974.

[13] Traci, R. M., Albano, E. D., and Farr, J. L., "Small Disturbance Transonic Flows About Oscillating Airfoils and Planar Wings," AFFDL-TR-100, Aug. 1975.

[14] Weatherill, W. H., Ehlers, R. E., and Sebastian, J. D., "Computation of the Transonic Perturbation Flow Field Around Two- and Three-Dimensional Oscillating Wings," AIAA Paper 76-99, Jan. 1976.

[15] Ballhaus, W. H. and Goorjian, P. M., "Implicit Finite-Difference Computations of Unsteady Transonic Flows About Airfoils," *AIAA Journal,* Vol. 15, Dec. 1977, pp. 1728-1735.

[16] Tijdeman, H., "Investigations of the Transonic Flow Around Oscillating Airfoils," NLR Report TR77090, Dec. 1977.

[17] Weatherill, W. H. and Ehlers, F. E., "Analysis of Transonic Flow About Harmonically Oscillating Airfoils and Wings," AIAA Paper 80-149, Jan. 1980.

[18] Ashley, H., "Role of Shocks in the 'Sub-Transonic' Flutter Phenomenon," *Journal of Aircraft,* Vol. 17, March 1980, pp. 187-197.

[19] Rizzetta, D. P. and Chin, W. C., "Effect of Frequency in Unsteady Transonic Flow," *AIAA Journal,* Vol. 17, July 1979, pp. 779-781.

[20] Caradonna, F. X. and Isom, M. P., "Numerical Calculation of Unsteady Transonic Potential Flow Over Helicopter Rotor Blades," *AIAA Journal,* Vol. 14, April 1976, pp. 482-488.

[21] Caradonna, F. X. and Phillippe, J. J., "The Flow Over a Helicopter Blade Tip in the Transonic Regime," *Vertica,* Vol. 2, 1978, pp. 43-60.

[22] Isogai, K., "Calculation of Unsteady Transonic Flow Over Oscillating Airfoils Using the Full Potential Equation," AIAA Paper 77-448, March 1977.

[23] Goorjian, P., "Implicit Computations of Unsteady Transonic Flow Governed by the Full Potential Equation in Conservation Form," AIAA Paper 80-150, Jan. 1980.

[24] Van der Vooren, J., Sloorf, J. W., Hizing, G. H., and Van Essen, A., "Remarks on the Suitability of Various Transonic Perturbation Equations to Describe Three-Dimensional Transonic Flow-Examples of Computations Using a Fully-Conservative Rotated Difference Scheme," *Symposium Transsonicum II,* Göttingen, West Germany, Sept. 1975; Proceedings, Springer-Verlag, Berlin, 1976, pp. 556-557.

[25] Borland, C. J. and Rizzetta, D. P., "Transonic Aerodynamics for Aeroelastic Applications," Vol. I, Technical Development Summary, AFWAL-TR-80-3107, May 1981.